Rheology of Dendrimers. 2. Bulk Polyamidoamine Dendrimers under Steady Shear, Creep, and Dynamic Oscillatory Shear

Srinivas Uppuluri,[†] Faith A. Morrison,[‡] and Petar R. Dvornic*[,†]

Michigan Molecular Institute, 1910 W. St. Andrews Road, Midland, Michigan 48640, and Department of Chemical Engineering, Michigan Technological University, Houghton, Michigan 49931

Received April 23, 1999

ABSTRACT: Rheological behavior of the first eight generations of bulk polyamidoamine (PAMAM) dendrimers, having nominal molecular weights from about 500 to over 116 000, was investigated under steady shear, shear creep, and dynamic oscillatory shear within the temperature range from $T_g + 15$ °C to $T_g + 105$ °C. It was found that these dendrimers exhibit (a) constant viscosity at small deformations regardless of the type of stress applied and (b) temperature-/generation-dependent non-Newtonian response at higher shear rates/frequencies. The latter was characterized by finite moduli of elasticity at all generations and by onset of complex-viscosity thinning at some generation-dependent critical temperature and shear frequency. These results represent the first observation of elasticity in one dendrimer family, and they indicate that at rest in bulk these dendrimers collapse, deform, and organize into transient, secondary (i.e., hydrogen)-bonded, quasi-network supramolecular microstructure. They also reveal a distinct change from single-relaxation-mode to a multirelaxation-mode Maxwell-type behavior at generation 4, which is consistent with the closure of dendrimer molecular surface upon itself and the earlier proposed soft interior−dense shell model of *intra*molecular dendrimer morphology. Further support for this model resulted from an analysis of dendrimer free volume, which exhibited significant contribution not only from the dendrimer end groups but also from their interior building blocks. To account for these observations, a model is proposed that involves dynamics of structural elements that are smaller than the overall dendrimer molecules.

Introduction

Recently we reported on a rheological study of the first seven generations of ethylenediamene (EDA)−core polyamidoamine (PAMAM) dendrimers in medium (30 wt %) to highly (75 wt %) concentrated ethylenediamine solutions.[1] It was found in that study that, over the entire range of shear rates and shear stresses applied, the examined dendrimer solutions showed Newtonian flow behavior with constant viscosities with respect to both shear rate and shear stress. It was also found that although the viscosities of these solutions increased with increasing dendrimer molecular weight (which ranged from about 500 at generation 0 to almost 60 000 at generation 6), this increase was neither similar to that typical for most traditional high molecular weight polymers (where zero-shear viscosity, η_0, scales with $M^{3.4}$) nor in accordance with the idealized Rousean prediction for nonentangled chains (where $\eta_0 \sim M^1$). Instead, the slopes of dendrimer solutions' log η_0 vs log M curves decreased with generation from about 2−3 between generations 0 and 1 to approaching unity above about generation 4. Since similar viscosity dependence on molecular weight (i.e., generation) was also found for bulk PAMAM[1] and poly(benzyl ether) (PBE) dendrimers,[2] we proposed[1] that this behavior may represent a characteristic property that is specific for the unique type of this macromolecular architecture and independent of dendrimer state (i.e., solution or bulk) and chemical composition.

In fact, the flows of both dendrimer solutions and bulks seem to be fundamentally different from the flows of all other types of polymers with more traditional molecular architectures,[3] and with a variety of other data on physical and chemical properties,[4,5] rheological behavior,[1,2,6−8] and computer simulations,[1,9,10] present a rather unique picture of these macromolecules. This picture suggests that in solutions low-generation members of the PAMAM dendrimer homologous series are open, domelike molecules that can easily interpenetrate and establish appreciable *inter*molecular interactions.[1,9] However, when they exceed a certain critical degree of branching at generation 2,[1,11] the crowding of end groups begins to require that their outer molecular surface closes upon itself, and *inter*dendrimer interpenetration becomes difficult if not completely impossible.[1,6] During this transformation, fully developed PAMAM dendrimers (i.e., generations 3−7) become spheroidal,[12,14] with soft and spongy interior and considerably denser, hard-shell exterior.[1,6] This outer shell is permeable to relatively small molecules (such as those of solvents or low-molecular-weight organic or inorganic substances)[6] but impenetrable to high-molecular-weight macromolecules[13] and/or other dendrimers or their parts.[6] As a consequence, such dendrimers adopt well-defined particle-like outer boundaries, which have been observed in small-angle X-ray and neutron scattering studies.[5,14]

However, although this hard shell−soft interior model of *intra*dendrimer morphology[6] can account for a pronounced flexibility of these molecules, which enables their expansion[1,4,6] and/or shrinking[15] depending on the solvent quality, solution concentration, and temperature, it seems improbable that dendrimers can sustain internal hollowness (i.e., softness) in the absence of solvent to fill their interior. Instead, it appears more realistic that in the bulk state higher generation dendrimers must flatten and/or collapse, considerably changing their shape, conformation, macroscopic prop-

[†] Michigan Molecular Institute.
[‡] Michigan Technological University.
* To whom correspondence should be addressed.

10.1021/ma990634u CCC: $19.00
Published on Web 03/11/2000

Table 1. Relative Molecular Weight, M_r,[a] Number of End Groups per Molecule, Z,[a] Bulk Density at 40 °C, ρ, and Glass Temperature, T_g, of the First Eight Generations of EDA−Core PAMAM Dendrimers

generation	M_r	Z	ρ (g/cm^3)	T_g (°C)
0	517	4	1.152	−11
1	1430	8	1.169	−3
2	3256	16	1.188	0
3	6909	32	1.187	11
4	14215	64	1.188	14
5	28826	128	1.195	14
6	58048	256		16
7	116493	512		

[a] Nominal values calculated assuming ideal divergent dendrimer growth. For more details see ref 11.

erties, and behavior, although there are also indications that even under such conditions their molecular interiors may remain surprisingly mobile. Such indications include the well-known universal shape of dendrimer glass temperature (T_g) vs generation dependence[4,16−18] and a pronounced ability of some dendrimer-based networks to accommodate low molecular weight guests inside their dendritic armature.[19−22] Hence, in an attempt to shed some light on this apparent controversy, in this work we examined the bulk rheology of the first eight generations of EDA−core PAMAM dendrimers under steady shear, shear creep, and dynamic oscillatory shear. However, due to the stability limitations of these dendrimers, the study was limited to temperatures ranging from T_g + 15 °C to T_g + 105 °C (i.e., to WLF conditions).[4,23] As a consequence, the results obtained do not represent a simple extension of the previously reported behavior of these same dendrimers in medium to highly concentrated solutions.[1]

Experimental Section

The first eight generations (i.e., generations 0−7) of ethylenediamine (EDA)−core polyamidoamine (PAMAM) dendrimers, obtained from Dendritech, Inc., Midland, MI, were used in this work. These dendrimers were prepared by the well-known excess-reagent, divergent-growth method, described in detail elsewhere in the literature,[11,24] and some of their relevant molecular and physical properties are listed in Table 1.

The samples were obtained as methanol solutions and were thoroughly dried before use until no residual solvent could be detected by thermogravimetric analysis (TGA). To verify their stability under the testing conditions, generation 3 was evaluated for hygroscopicity and mechanical resistance. For this purpose, two identical rheological scans were performed: one with bare sample and another with a sample protected with a low-viscosity, poly(dimethylsiloxane) blanket. The difference between the viscosity values obtained from these two runs was less than 3%, which was the same as the difference between the viscosity values measured on the blanketed sample immediately after loading into the instrument and after 5 h of testing.

Measurements were performed using a TA Instruments Carri-Med CSL^2 500 controlled-stress rheometer with a cone-and-plate geometry. The instrument was calibrated with three different poly(dimethylsiloxane) viscosity standards obtained from Dow Corning Corp. and having declared zero-shear kinematic viscosities of 1000 cSt, 60 000 cSt at 25 °C, and 270 000 cSt at 20 °C. This calibration confirmed the manufacturer-declared maximum error of the viscometer of ±5%. For lower-generation dendrimers, a 2° angle and 4 cm diameter cone were used, while generations 5 and 6 were evaluated with a cone having 1° angle and 2 cm diameter. The data were collected using Version 5.0 Carri-Med software for the CSL rheometers, and the experiments were performed at regular 10 °C intervals within the temperature range from 40 to 70 °C and at 5 °C intervals within the temperature range from 70 to 95 °C. Temperature was maintained within ±0.3 °C using a Peltier temperature control system. This temperature range was chosen because of dendrimer thermal and thermooxidative instability at temperatures above about 120 °C[4] and out-of-instrument-range viscosities for higher generations at lower temperatures. To account for thermal expansion of the rheometer parts, the gap between the cone and the plate was computer-controlled at all temperatures to 52 μm for the 4 cm diameter cone and to 26 μm for the 2 cm diameter one.

The samples were subject to steady shear, shear creep, and dynamic oscillatory stressing (small-amplitude oscillatory shear, SAOS). In the steady-shear mode, the applied stress range was ramped between 50 and 29 000 dyn/cm^2, with logarithmic increments in 2 min intervals, and sweeps of both increasing and decreasing shear rates were recorded. In creep experiments, the samples were subject to stress at time zero, and the compliance was monitored at constant stress for 2 min, at which time the applied stress was removed, and the relaxation behavior was recorded. This procedure was followed at various stresses within the range from 100 to 29 000 dyn/cm^2. For generation 6, which showed evidence of creep recovery at lower stresses and temperatures, the run was extended to the next higher stress, and this was repeated until nine different stresses were covered within the above stress range. The sequence of stresses used in this case was 100, 500, 1000, 5000, 10 000, 20 000, 25 000, and 29 000 dyn/cm^2. For all other samples, measurements were made at only two stresses of 100 and 15 000 dyn/cm^2. These measurements were carried out at regular 5 °C intervals from 70 to 95 °C.

In the SAOS experiments, the range of frequencies covered was from 0.1 to 220 rad/s. Before applying a frequency sweep, each sample was tested at each temperature to determine the range of its linear viscoelastic response (LVR). The tests were performed by stress sweeping at constant frequency, and the LVR range was determined as the region where true sinusoidal response was observed; the storage and loss moduli (G' and G'') were constant (i.e., within ±5%) over the entire range of stress. After establishing the LVR stress region at different frequencies, a range of frequencies corresponding to the LVR was selected for sample evaluation, and the frequency sweeps were performed within a temperature range from 40 to 95 °C. A 2% strain was used in all frequency sweeps. In the case of generation-0 PAMAM, the angular velocity exceeded the instrument capability at temperatures above 80 °C, so that the tests were performed only between 40 and 80 °C. For generation-5 dendrimer at 95 °C, there was no linear viscoelastic response observed at and below 50 rad/s or above 150 rad/s; hence, this sample was tested only between 40 and 90 °C. For the same reason, generation-6 dendrimer was tested only between 50 and 95 °C. A constant value of 0.065 in tan δ was subtracted from all data to account for an instrument offset.

Once loaded into the rheometer, the same samples were used for all three types of stress measurements performed: steady shear, shear creep, and dynamic oscillatory shear. At the end of each experiment the stability of the sample was tested by repeating the steady-shear viscosity at 70 °C and comparing the result obtained with the value determined under the same testing conditions immediately after initial sample loading. For all samples this difference did not exceed ±5%, except for generation-2 dendrimer where it was +9%.

Complex viscosities of generation-7 dendrimer were measured within the temperature range from 70 to 95 °C using a Rheometrics RMS-605 equipped with a cone having a diameter of 12.5 mm and an angle of 0.8°. This sample was not characterized more extensively on the Carri-Med, since its viscosity exceeded the measurement range of that instrument.

Results and Discussion

Creep and Steady Shear. In creep experiments, generations 0−5 PAMAMs showed ideal viscous behavior at all applied stresses and over the entire range of

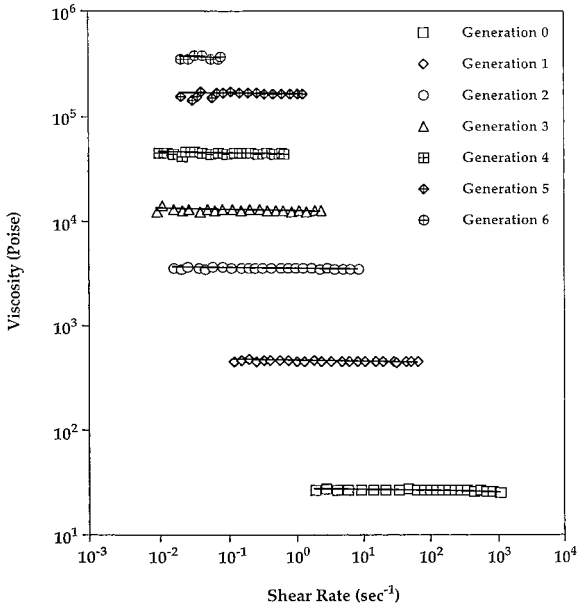

Figure 1. Steady shear viscosity as a function of shear rate for the first seven generations of bulk EDA−core PAMAM dendrimers at 70 °C.

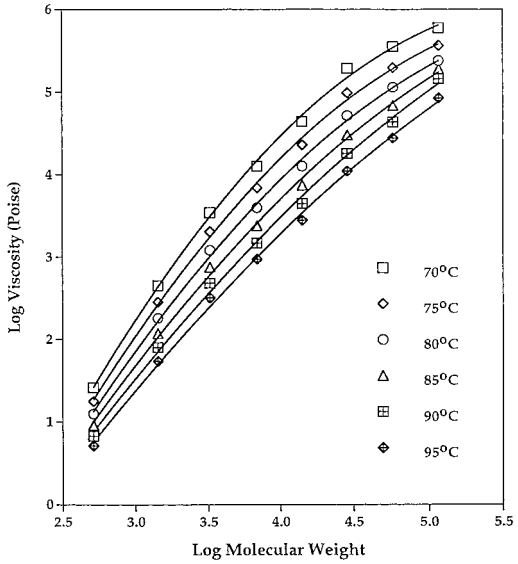

Figure 2. Steady shear viscosity as a function of molecular weight for bulk EDA−core PAMAM dendrimers at indicated temperatures. For values of slopes and their dependence on molecular weight (i.e., generation) and temperature, see Table 2.

testing temperatures.[4] Accordingly, under steady shear, generations 0−6 showed constant viscosity over the entire range of applied stresses and shear rates, as illustrated in Figure 1 for an arbitrarily selected temperature of 70 °C. In no case did the plots of shear stress vs shear rate obtained from the forward and from the reverse sweep show hysteresis, indicating absence of thixotropy in these fluids. For generation 0, however, the viscosity was so low at higher temperatures that angular velocity exceeded the limit of the instrument, and the reverse sweep could not be performed.

The dependence of steady-shear viscosity on molecular weight for generations 0−7 at various experimental temperatures is shown in Figure 2. It can be seen from this figure that while the shapes of the obtained curves clearly depended on temperature, their slopes steadily decreased with molecular weight (i.e., generation) at all

Table 2. Slopes of log(steady-shear viscosity) vs log(molecular weight) Relationships of Bulk EDA-core PAMAM Dendrimers as a Function of Generation and Temperature

	slope between generations						
generation	0−1	1−2	2−3	3−4	4−5	5−6	6−7
70 °C	2.8	2.5	1.7	1.7	2.1	0.9	0.8
75 °C	2.7	2.4	1.6	1.7	2.1	1.0	0.9
80 °C	2.6	2.3	1.6	1.6	2.0	1.1	1.1
85 °C	2.5	2.3	1.5	1.6	2.0	1.2	1.5
90 °C	2.4	2.2	1.5	1.5	2.0	1.3	1.7
95 °C	2.3	2.2	1.4	1.5	2.0	1.3	1.6

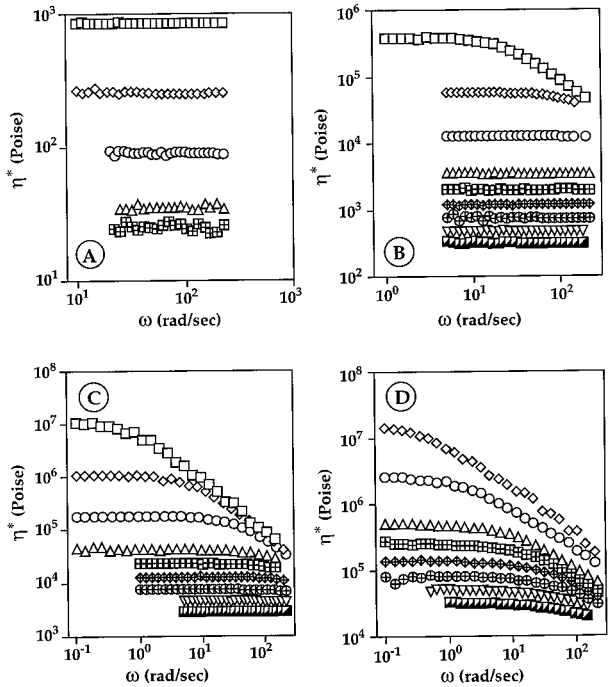

Figure 3. Complex viscosity as a function of shear frequency for bulk EDA−core PAMAMs of generation 0 (A), 2 (B), 4 (C), and 6 (D) at 40 (squares), 50 (diamonds), 60 (circles), 70 (triangles), 75 (squares with + marks inside), 80 (diamonds with + mark inside), 85 (circles with + mark inside), 90 (inverted triangle), and 95 °C (half-filled squares).

temperatures, and the magnitude of this decrease increased with decrease in temperature (see Table 2). Notably, this behavior was identical to that previously found for these same dendrimers in medium and highly concentrated solutions,[1] as well as for both PAMAM[1] and PBE[2] dendrimers in bulk, but at the same time, it was dramatically different from the well-known, broken-linear log η_0 vs log M_w relationship of traditional linear polymers.[25] This important difference was particularly clear in the direct comparison of the behavior of these PAMAM dendrimers and their linear counterparts of the same chemical composition and comparable molecular weights.[1]

Small-Amplitude Oscillatory Shear. In contrast to the above-described constant-viscosity behavior under steady shear, these same bulk PAMAMs responded to dynamic oscillatory shearing by exhibiting quite pronounced frequency dependence of complex viscosities, as illustrated for selected generations in Figure 3. It should be noted that this represents the first observation of complex viscosity thinning in a dendrimer system,[1,2,8] including solutions of these same PAMAMs in which dendrimer concentration was as high as 75 wt %.[1]

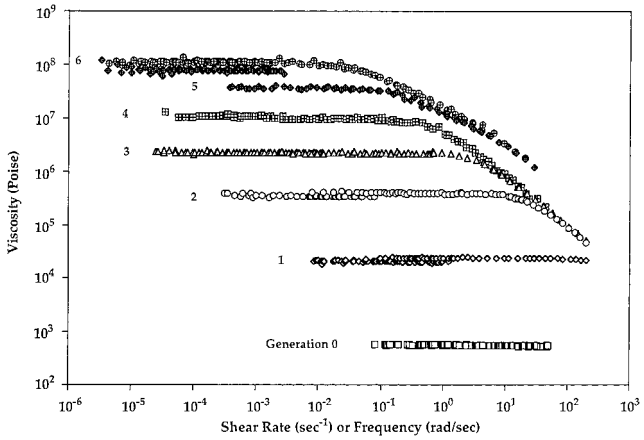

Figure 4. Master curves of steady shear (η) (at lower shear rate values) and complex (η^*) (at higher frequency values) viscosities as a function of shear rate ($\dot{\gamma}$) or frequency (ω) for the first seven generations of bulk EDA−core PAMAM dendrimers at arbitrarily selected reference temperature of 40 °C.

As shown in Figure 3, the onset of this frequency dependence of complex viscosity was a function of temperature and dendrimer generation. In principle, this behavior may be due to the proximity of glass temperatures or to some kind of supramolecular dendrimer structuralization in the state of rest. However, since dendrimers should be expected to respond to higher shearing frequencies just as to lower temperatures, at any chosen frequency higher-generation dendrimers would be closer to their glass temperatures than the lower-generation ones and should, therefore, show more elastic behavior than the latter. Hence, it seems more likely that the observed complex-viscosity thinning and its temperature dependence are caused by the proximity of generation-dependent T_g than by *inter*dendrimer interactions of the entanglement type. Nevertheless, this does not preclude some sort of supramolecular microorganization of deformed (i.e., flattened or collapsed) dendrimers in the state of rest. Such organization may result from compositionally dependent secondary interactions, which in the case of PAMAMs may involve *inter*dendrimer hydrogen bonding.

Time−Temperature Superposition. The results obtained from steady and oscillatory shear experiments could be time−temperature superposed,[26] permitting construction of master curves at an arbitrarily chosen reference temperature, T_0, as shown in Figure 4. For steady-state viscosities, η, this was accomplished by multiplying experimental viscosities with appropriate shift factors $a_T(T) = \eta(T)T_0\rho_0/\eta(T_0)T\rho_T$, where $\eta(T)$ is the viscosity at temperature T, $\eta(T_0)$ is the viscosity at reference temperature T_0, and ρ_T and ρ_0 are densities at temperatures T and T_0, respectively. For complex viscosities, η^*, the shifts were performed by translating experimental G' and G'' vs ω curves until good superposition was achieved, and a_T^* was calculated subsequently. It was observed (as shown in Figure 5) that the shift factors obtained from steady-state viscosities, a_T, and from complex viscosities, a_T^*, were identical for generations 0−3 and for generation 6, while differences appeared for generation 4 and particularly for generation 5. The reason(s) for these differences are not clear from these data alone.

It can be also seen from Figures 3 and 4 that in general the empirical Cox−Merz rule[27] holds for PAMAMs so that the steady-shear and complex viscosities

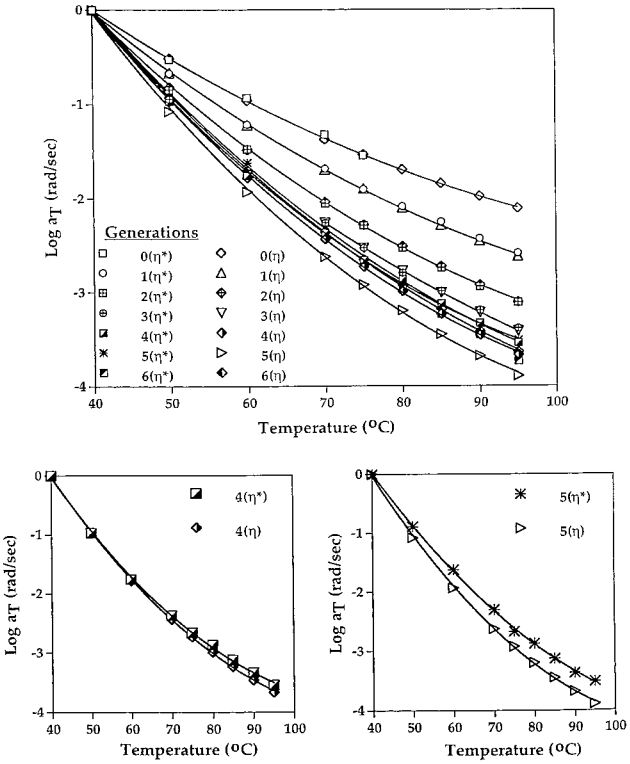

Figure 5. Temperature dependence of shift factors for bulk EDA−core PAMAMs. Curves for generations 4 and 5 are also shown isolated in order to illustrate the observed discrepancies between the values obtained from steady-state and complex viscosities as discussed in the text. Solid lines indicate a fit of each curve to the WLF equation.

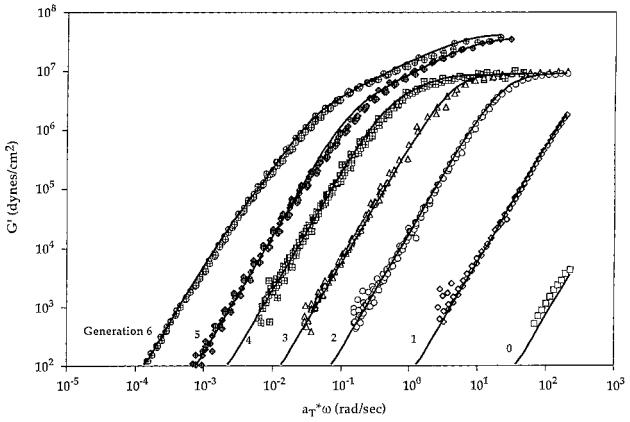

Figure 6. Elastic component of the dynamic modulus of bulk EDA−core PAMAM dendrimers of indicated generations as a function of shifted shear frequency ($a_T^*\omega$) at a reference temperature of 40 °C. Solid lines indicate a fit of each curve to the generalized Maxwell model.

are equal when compared at numerically equal shear rates and angular frequencies (i.e., $\eta(\dot{\gamma}) = \eta^*(\omega)$, where $\dot{\gamma} = \omega$). Once again, however, as with the shift factors, generation 5 was the only notable exception to this rule. It should be noted, however, that the overlap of $\dot{\gamma}$ and ω was less than 1.5 decades and did not extend into the complex-viscosity-thinning region of ω.

Moduli of Bulk Dendrimers. Master curves for storage (G') and loss (G'') moduli of all examined bulk PAMAMs at the reference temperature $T_0 = 40$ °C are shown in Figures 6 and 7, respectively. For generations 0−3 these curves very closely conformed at all frequen-

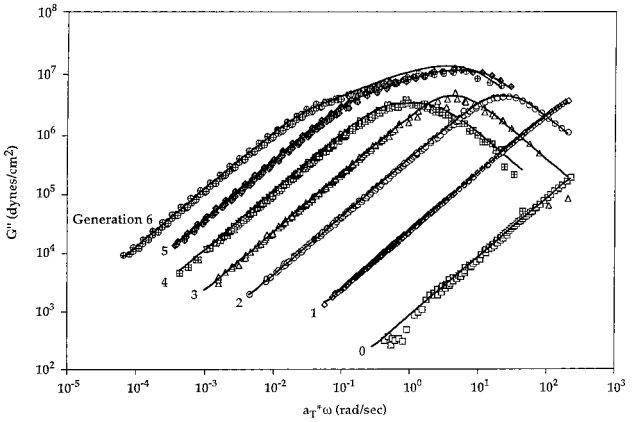

Figure 7. Loss component of the dynamic modulus of bulk EDA−core PAMAM dendrimers of indicated generations as a function of shifted shear frequency ($a_T{*}\omega$) at a reference temperature of 40 °C. Solid lines indicate a fit of each curve to the generalized Maxwell model.

cies to the classic shape of a single-relaxation-time Maxwell model, described by the following equation:

$$\lambda_0 \frac{\partial \tau}{\partial t} + \tau = -G_0 \lambda_0 \dot{\gamma} \tag{1}$$

where τ is the stress tensor, $\dot{\gamma}$ is the shear rate tensor, t is time, λ_0 is the relaxation time, and G_0 is a modulus parameter. Since the Maxwell model predicts constant steady-shear viscosity (η) with shear rate, this is also consistent with the steady-shear data of Figure 1.

For higher generation dendrimers (i.e., generations 4−6), however, the single-relaxation-time Maxwell model failed to provide adequate fits for the measured data. Instead, excellent fits were obtained when the model was generalized to include multiple relaxation times representing a spectrum of mobility modes. The spacing of the modes was consistent with the prediction of the Rouse model[26,28] and is described by the following set of equations:

$$\tau = \sum_{k=1}^{N} \tau_k \tag{2}$$

$$\lambda_k \frac{\partial \tau_k}{\partial t} + \tau_k = -G_0 \lambda_k \dot{\gamma} \tag{3}$$

$$\lambda_k = \frac{\lambda_0}{k^2} \tag{4}$$

where τ_k and λ_k are the individual stress contribution and the relaxation time of the kth mode, λ_0 is the longest relaxation time, and N is the number of different mobility modes used. While for generation 4 only two mobility modes were needed to fit the data well (i.e., $N = 2$), for generations 5 and 6, $N = 9$ and $N = 15$ modes were necessary, and generation 6 required yet another (16th) non-Rousean low-frequency mode, $\lambda_{\text{ultralow}} = 280$ s, $G_{0,\text{ultralow}} = 4 \times 10^4$ dyn/cm^2, to adequately reflect the shapes of G' and G'' at low frequencies. This was necessary because in the low-frequency (terminal) zone G' and G'' scaled with $\omega^{1.49}$and $\omega^{0.92}$, respectively, while the generalized Maxwell model requires $G' \sim \omega^2$ and $G'' \sim \omega^1$ in the terminal zone. In Figures 6 and 7, the model fits are shown as solid lines, while the values of the relaxation times (λ_0) and modulus parameters (G_0) used are listed in Table 3. It can be seen from this table that G_0 values were essentially identical for generations 0−3, which is consistent with the common high-frequency values of the storage modulus, and almost identical heights of the maxima of the loss modulus of generations 2−4, as shown in Figures 6 and 7, respectively.

Table 3. Values of the Longest Relaxation Times, λ_0, and Moduli, G_0, Used To Fit Experimental Linear Viscoelastic Data of PAMAM Dendrimers at 40 °C as Described in the Text

generation	M_r[a]	λ_0 (s)	$10^{-6}G_0$ (dyn/cm^2)
0	517	0.000085	10
1	1430	0.0025	9.2
2	3256	0.044	9.2
3	6909	0.24	9.2
4	14215	2	4.4
5	28826	6	4.0
6	58048	25	2.8

[a] See note to Table 1.

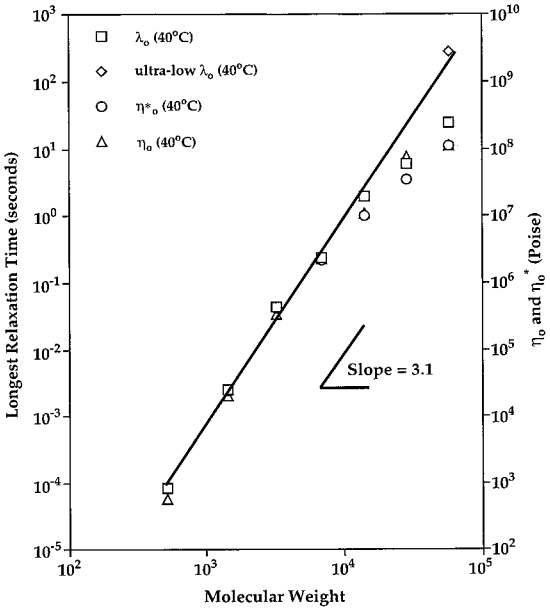

Figure 8. Comparison of the molecular weight dependencies of the longest relaxation times (λ_0 and ultralow λ_0) and complex ($\eta_0{*}$) and steady-shear (η_0) viscosities of bulk EDA−core PAMAMs at a reference temperature of 40 °C. Note that the solid line drawn has the slope of 3.1.

From generation 0 to 4, the longest relaxation time, λ_0, increased at the selected reference temperature as $\lambda_0 = M^{3.1}$, as shown in Figure 8. In addition, this increase matched very closely the increase of steady-shear viscosity (η_0) and zero-frequency complex viscosity ($\eta_0{*}$) with molecular weight, but above that generation the two relationships began to diverge. Note, however, that since the shift factors were not the same for all generations (see Figure 5), the slope of the η_0 vs M relationship was dependent on the choice of the reference temperature (compare with data of Table 2). Also, the divergence of λ_0 vs M and η_0 vs M at high generations is consistent with the fact that multimode relaxation spectra were needed to fit the higher generation data. Curiously, if the value for the relaxation time of the 16th, ultralow-frequency mode used to fit the low-frequency portion of the generation-6 data is also included in Figure 8, it falls almost perfectly on the scaling line defined by the lower-generation dendrimer data.

It should be noted that although the longest relaxation times were calculated by using fits to the time−temperature superimposed moduli, the observed behavior is consistent with the directly measured viscosity data of Figure 2 and Table 2. Thus, the slope of the λ_0 vs molecular weight relationship of Figure 8 decreases with generation just as the slopes of the measured viscosity vs molecular weight curves decrease, showing considerable internal consistency of the data. A more detailed discussion of possible physical reason(s) for this behavior is presented in our previous publication.[1]

It is interesting to compare the linear viscoelastic responses of generation-5 and -6 PAMAM dendrimers and polymer stars. For both of these two types of macromolecular architecture, the crossover of G' and G'' does not occur at $\omega\lambda_1 = 1$, which is the predicted value for a single-relaxation-time Maxwell fluid and which was experimentally found for the lower-generation dendrimers in this work. Instead, at the crossover $\omega\lambda_1$ is 4 for stars (independent of the number of branches[29]), 4.8 for generation-5, and 7.5 for generation-6 PAMAM dendrimers. In addition, the magnitude of G' at the crossover is independent of molecular weight for these two generations of PAMAM dendrimers, similar to what is generally found for linear polymers, while for stars the value of G' at the crossover decreases with approximately the reciprocal of the arm molecular weight.[29] Thus, although both stars and high-generation dendrimers are more compact macromolecules than loose random-coil linear polymers, the similarity ends here as they exhibit qualitatively different characteristics in SAOS.

Free Volume in Bulk PAMAM Dendrimers. In the rheology of traditional polymer architectures, the temperature dependence of the shift factors used to obtain master curves for complex, η^*, and steady-shear viscosities, η, can be represented either by a WLF equation,[30] if the selected reference temperature is close to the polymer T_g, or by an Arrhenius-type relationship,[31] if this temperature is far enough above T_g (i.e., usually at least 100 °C). Since all temperatures at which experimental measurements were performed in this work were relatively close to the PAMAMs' glass temperatures (see Table 1), the WLF eq 5 was used to fit $a_T(T)$.

$$\log a_T = -C_1^\circ(T - T_0)/[C_2^\circ + (T - T_0)] \qquad (5)$$

In this equation $C_1^\circ = B/2.303f_{ref}$ and $C_2^\circ = f_{ref}/\alpha_f$, where the reference free volume, f_{ref}, is taken to be f_0, the free volume at $T_0 = 40$ °C, and α_f is the thermal expansion coefficient at the same reference temperature. Values of C_1° and C_2° were obtained by the least-squares method from the slope and intercept of the linear fits of $(T - T_0)/\log a_T$ vs $(T - T_0)$ and are listed in Table 4. From the values of C_1°, the fractional free volumes, f_0, were calculated assuming $B = 1$,[32] and the results are also listed in Table 4 and shown as a function of dendrimer generation (i.e., molecular weight) in Figure 9. Errors involved in these calculations were determined using the maximum and minimum slopes and corresponding intercepts that fit within a 95% confidence interval on the *linear* $(T - T_0)/\log a_T$ vs $(T - T_0)$ plots where for all generations both $a_T(T)$ and $a_T^*(T)$ were combined to perform the fit. For generation 5 only, this procedure resulted in a relatively large error because of the differences encountered between $a_T(T)$ and $a_T^*(T)$.

Table 4. Values of WLF Parameters, C_1°, C_2°, Fractional Free Volumes f_0 and f_g, and Thermal Expansion Coefficient, α_f, for the First Seven Generations of EDA−Core PAMAM Dendrimers

generation[a]	M_r	C_1°	C_2° (K)	f_g/B	$10000\alpha_f/B$	f_0/B
0	517	6.7	120	0.037	5.4	0.065
1	1430	7.5	102	0.034	5.7	0.058
2	3256	8.2	90	0.029	5.9	0.053
3	6909	8.9	84	0.026	5.8	0.049
4 (η)	14 215	9.5	87	0.032	5.2	0.046
4 (η^*)	14 215	9.5	87	0.032	5.2	0.046
5 (η)	28 826	9.3	76	0.031	6.1	0.047
5 (η^*)	28 826	9.3	86	0.033	5.4	0.047
6 (η)	58 048	10.4	101	0.031	4.1	0.042
6 (η^*)	58 048	10.4	101	0.031	4.2	0.042

[a] For generations 4−6, two sets of values for a_T were obtained from steady shear (η) and complex (η^*) viscosity data (compare with Figure 5).

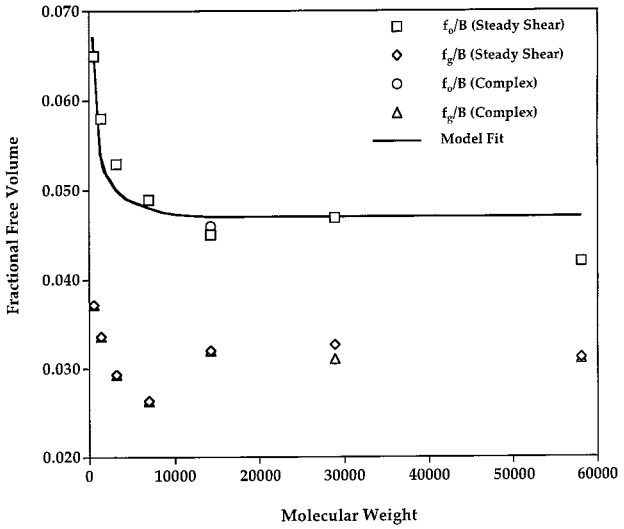

Figure 9. Fractional free volume as a function of molecular weight (i.e., generation) for bulk EDA−core PAMAM dendrimers at $T_0 = 40$ °C. Squares represent f_0/B values, diamonds f_g/B values, and the line results from the model discussed in the text. Empty and filled symbols were obtained from complex and steady-shear viscosity data, respectively.

It can be seen from Figure 9 that fractional free volume at 40 °C initially rapidly decreased with increasing molecular weight (i.e., generation), but then the decrease considerably slowed between generations 3 and 6 in a reasonable agreement with the leveling off of these same dendrimers' glass temperatures, which are expected to depend on free volume and which reach an asymptotic value of about 15 °C around generation(s) 3 and 4 (see Table 1).[4,11]

Values of the fractional free volumes at the glass temperature, f_g, were calculated from eq 6[26] and are also presented in Table 4 and shown in Figure 9.

$$f_g = f_{ref} + \frac{1}{2.303C_1^\circ}(T_g - T_{ref}) \qquad (6)$$

It can be seen from these data that, as is usually found for linear polymers, the f_g of PAMAMs was independent of molecular weight within experimental accuracy. Numerically, it was equal to 0.032 ± 0.006, which is somewhat higher than the value of 0.025 ± 0.005[33] found for many linear polymers but is identical to the value recently reported for PBE mono- and tridendron dendrimers[8] and a number of linear polymer exceptions,

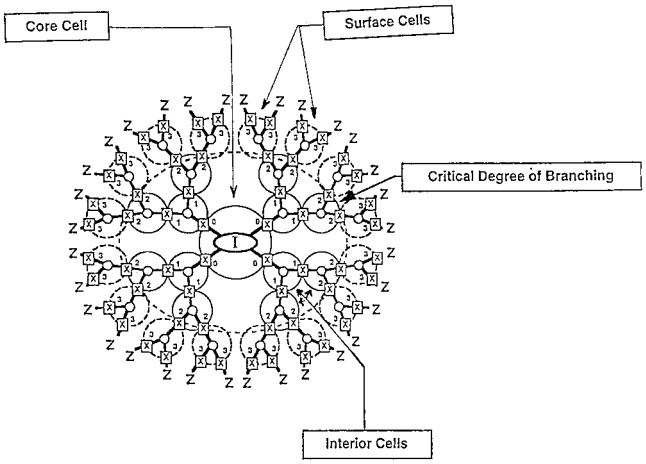

Figure 10. A schematic representation of planar projection of a tetradendron dendrimer. Note the three basic building blocks of dendrimer structure: the core cell, the interior cells, and the exterior cells. Straight lines between the neighboring branch junctures represent brunch juncture connectors (i.e., linear $-CH_2-CH_2-C(O)-N(H)-CH_2-CH_2-$ units in the PAMAM case). Also note that a branched molecule becomes a fully developed dendrimer only when it contains all three of these elements, i.e., when it grows over a critical development stage defined by the critical degree of branching.[1] Molecules below this critical development stage represent simply branched dendrimer precursors.

including, for example, polystyrene and ethylene–propylene copolymer.[34] Although it remains an open question whether this observation supports the concept of the glass temperature as an iso-free-volume state, it certainly seems significant that almost identical f_g values were obtained for different chemical compositions and, even more importantly, for very different macromolecular architectures.

For linear polymers, the molecular weight dependence of the fractional free volume can be represented as follows:

$$f(T,M) = f_\infty(T) + \frac{A}{M} \tag{7}$$

where f is fractional free volume at given temperature and molecular weight, f_∞ is fractional free volume at the same temperature and infinite molecular weight, M is molecular weight, and A/ρ is the molar free volume associated with the pairs of molecular ends (free volume/moles of pairs of free ends), where ρ is the density. Thus, f varies with $1/M$, reaching a constant value at high molecular weight where the free volume associated with end groups becomes insignificant in contribution to the total free volume. For dendrimers, however, this equation is not expected to hold because the number of end groups increases in a geometrically progressive manner with generation,[8,17] so that at every dendrimer generation fractional free volume associated with end groups contributes to the total free volume of the molecule together with the free volume associated with the core cell and the free volume associated with interior branch cells (see Figure 10).

Hence, the fractional free volume for dendrimers may be represented by the following equation:

$$f(M) = (\rho/M)(V_{core} + V_{internal}N_{internal} + V_{external}N_{external}) \tag{8}$$

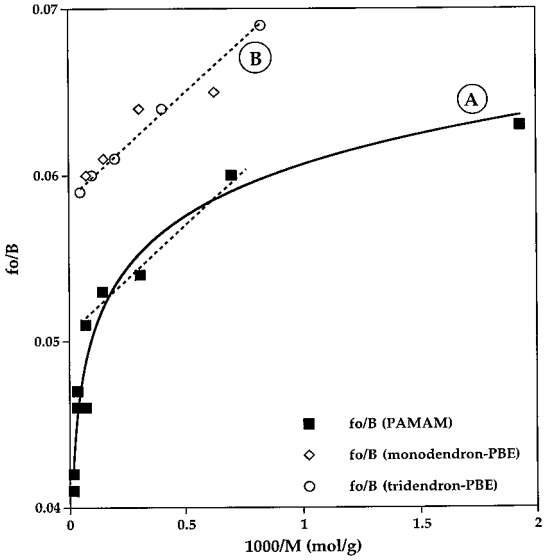

Figure 11. Comparison of the molecular weight dependence of the fractional free volume (f_0/B) of bulk tetradendron PAMAMs, tridendron PBEs, and monodendron PBEs. Data for PBEs were taken from ref 8. Solid line indicates a fit to the model discussed in the text.

where ρ is the density, M is molecular weight, V_{core}, $V_{internal}$, and $V_{external}$ are molar volumes of the core branch cells, interior branch cell, and exterior branch cells, respectively, while $N_{internal}$ and $N_{external}$ are the corresponding numbers of interior and exterior branch cells per dendrimer molecule, with the number of core branch cells equal to unity.

This equation gives for bulk PAMAM dendrimers curve A of Figure 11, which can be compared with the straight line relationship (B of the same figure) that Farrington and co-workers recently reported for PBE dendrimers.[8] It can be seen that, over the intermediate range of $1000/M$ between about 0.7 and 0.065 (i.e., between molecular weights of about 1500 and 15 000, respectively), both of these dendrimer families showed a reasonably straight linear $f(1/M)$ relationship (compare dashed lines in Figure 11), while for both lower and higher values of $1/M$, where only data for PAMAMs are available, this relationship is clearly and significantly curved, particularly at the high-generation end (i.e., at lower $1/M$ values). The least-squares fit to eq 8 using $\rho V_{core} = 7.1$, $\rho V_{internal} = 3.7$, and $\rho V_{external} = 6.9$, shown as curve A in Figure 11 and also as the model fit in Figure 9, is within experimental uncertainty for all generations.

An alternate way of considering the change of f_0 with generation may be as a function of generation number, assuming that it represents some measure of the molecular size. Plotted this way, f_0 of bulk PAMAMs decreased along a straight line having a slope of -0.0035 and an intercept of 0.0619. The sums of the squares of the deviations between the experimental data and molecular weight model (5.8×10^{-5}; eq 8) and this linear generation-number fit (3.0×10^{-5}) were similar, and both models gave predictions that were within the experimental uncertainty of the data.

Thermal Expansion Coefficient of Bulk PAMAM Dendrimers. Values of the thermal expansion coefficient, α_f, obtained for bulk PAMAM dendrimers from WLF shift factors and C_2^o are also listed in Table 4. It can be seen from this table that within experimental uncertainty α_f was constant with molecular weight. The

average value of α_f/B was 5.3×10^{-4} with a residual standard deviation of 7×10^{-5}. This trend was identical to that earlier found for PBE mono- and tridendron dendrimers,[8] except that α_f/B values for the latter were somewhat higher and ranged between 7.1×10^{-4} and 8.5×10^{-4}.

Flow Dynamics of Bulk Dendrimers. The appearance of finite elastic moduli, G', for all examined dendrimers (see Figures 6 and 7 keeping in mind that $G' = 0$ for Newtonian fluids) and the temperature/generation-dependent complex-viscosity thinning (see Figures 3 and 4) observed in this study for bulk PAMAMs have not been seen in any other previous examination of a dendrimer system, including medium to highly concentrated solutions of these same dendrimers[1] and bulk PBEs.[2,8] This is particularly intriguing with respect to the latter because while the observed differences between Newtonian PAMAM solutions and non-Newtonian PAMAM bulks could be ascribed to differences in their states relative to glass temperatures (i.e., while the solutions were examined under typical Arrhenius-type conditions, the bulks were tested within the WLF region), bulk PBEs were examined under comparable conditions, including the $T-T_g$ intervals of between 2 and 140 °C, nominal dendrimer molecular weights of between 320 and 84 219, and oscillatory shear between 0.1 and 100 rad/s.[2,8] Therefore, the appearance of elasticity in bulk PAMAMs seems to suggest that, in contrast to their solutions,[1] significant *inter*molecular interactions (probably through extensive secondary hydrogen bonding) occur in the bulk, leading to the formation of some kind of supramolecular microstructure, or a transient quasi-network capable of elastic deformation when exposed to external stress. At rest, this situation would become similar to what is often found in colloids or small-sphere dispersions, where attractive *inter*particle forces often lead to aggregation of small particles into larger clusters.[35]

At the molecular level, the deformation may involve elastic stretching of rheologically active structural elements that could range in size from branch-juncture connectors to entire main dendrons or to whole dendrimers, as depicted in Figure 10. Hence, even if in the state of rest these molecules collapse, filling the soft and spongy[6] dendrimer interior,[36] on exposure to stress they should be able to elongate in the stressing direction and to undergo extension away from the core. The resulting opening and deformation of the overall molecules may then allow them to interact with hydrogen-bonding neighbors, as illustrated in Figure 12.

To identify the rheologically active substructure(s) that could participate in such a deformation mechanism, it was attempted to fit the experimental data to the elastic dumbbell model,[37] which applies to single-relaxation-mode Maxwell fluids. In this model, the rheologically active element is a single dumbbell consisting of two beads and a connecting elastic spring, in which the spring provides an elastic restoring force, and the drag on the beads accounts for the viscous component of sustained deformation. The modulus of such a dumbbell, G_0, is given by νkT where ν is the number of dumbbells per unit volume, k is Boltzmann's constant, and T is the absolute temperature, while the dumbbell relaxation time, λ_0, is given by

$$\lambda_0 = \frac{\zeta}{4\kappa} \tag{9}$$

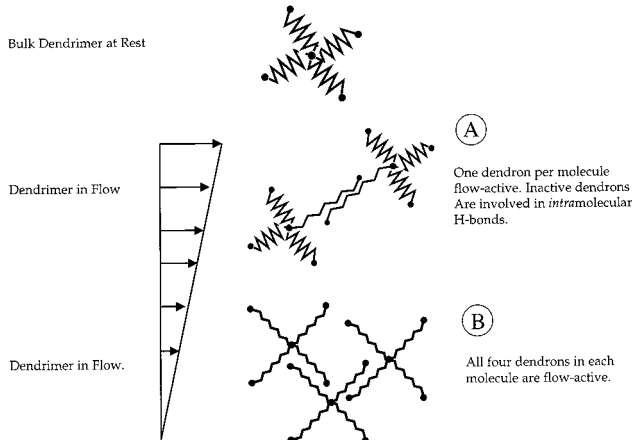

Figure 12. Schematic representation of possible *inter*dendrimer interactions that may occur on flow if only one dendron (A) or all four dendrons (B) of a tetradendron dendrimer is/are shear active.

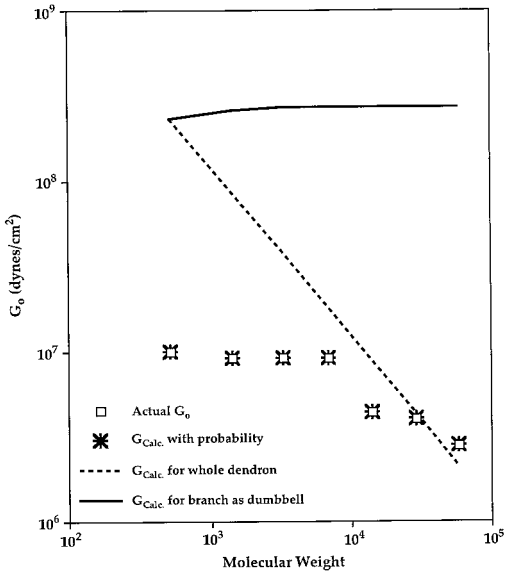

Figure 13. Molecular weight dependence of the generalized Maxwell model modulus parameter, G_0. Also shown are the predictions of $G_0(M)$ from various models discussed in the text.

where ζ is the bead-friction parameter (representing the total friction on the dumbbell) and κ is the spring constant.

If each dendron of a dendrimer molecule represents one dumbbell, for tetradendron (i.e., EDA core) PAMAM dendrimers the number of dumbbells per unit volume, ν, would be equal to $4\rho N_A/M$ (where ρ is the bulk density and N_A is Avogadro's number), and the modulus parameter (G_0) would be $G_0 = \nu kT = [4\rho N_A/M]kT$ (i.e., expected to scale with M^{-1}). As shown in Figure 13, for generations 0−3, G_0 was independent of molecular weight (i.e., $G_0 \sim M^0$), and a decrease with M^{-1} was found only between generations 5 and 6. Thus, this model captures the molecular weight dependence of G_0 for generations 5 and 6 in both magnitude and trend, while for generations 0−3 the values of G_0 were up to an order of magnitude lower than those calculated. This indicates that in lower-generation dendrimers entire dendrons *do not* act as individual dumbbells.

The situation for the low-generation dendrimers is reminiscent of what is usually found in the rheology of entangling linear polymers, where the appearance of a plateau modulus independent of molecular weight is

generally associated with the establishment of an entanglement network within which the stress-bearing elements are the segments between the entanglement loci, which are shorter than the individual chain.[28,38] For the low-generation dendrimers, therefore, the observed constant modulus may indicate that stress is being borne by molecular segments that are smaller than a single dendron, although the identity of these stress-bearing elements cannot be determined from these data alone.

Conclusions

The results obtained in this work revealed rather unexpected viscoelastic flow behavior of bulk PAMAM dendrimers that had not been observed before, either in the concentrated solutions of these same dendrimers or in their bulk poly(benzyl ether) counterparts. This behavior included (a) constant viscosity flow at small deformations, regardless of the type of stress applied (i.e., steady shear, shear creep, or oscillatory shear), and (b) non-Newtonian, viscoelastic response in SAOS at higher shear frequencies. The latter was characterized by (i) finite modulus of elasticity at all generations and (ii) complex-viscosity thinning at some generation-dependent critical temperature and shear rate/frequency.

At all temperatures and generations studied, the Newtonian region was characterized with zero-shear viscosities that were related to molecular weights in a manner that was identical in trend to that found earlier for the viscosities of medium to highly concentrated solutions of these same PAMAMs.[1] In both cases, the slopes of the monotonically increasing log η_0 vs log M relationships decreased with generations, approaching unity above about generation 4. Since the same was also found for bulk PBE dendrimers,[2] these results support our earlier suggestion that this behavior may represent one of the fingerprint properties of dendrimers that is specific for this unique type of macromolecular architecture and independent of the dendrimer state and chemical composition.[1]

An analysis of the temperature/generation-dependent viscoelasticity of bulk PAMAMs by both single- and multimode Maxwell models suggests that, in the state of rest, their deformed, collapsed molecules organize into transient, secondary (i.e., hydrogen)-bonded supramolecular microstructures. Unfortunately, due to limitations in thermal stability of PAMAMs, it was not possible to deduce whether this phenomenon is associated with the dendrimer bulk state in general or (more likely) with the proximity of glass temperatures in particular.

Qualitative changes in linear viscoelasticity were observed at dendrimer generation 4. While the lower molecular weight homologues showed excellent fit with the predictions of a single-relaxation-mode Maxwell model, generation 4−6 dendrimers were much better represented by multimode Maxwell models following a truncated Rouse spectrum. This change in behavior is consistent with the view that at about this generation a qualitative change in molecular conformation may occur, similar to what had been observed for the same dendrimers in solutions.[1] It was also noted that at very low frequencies generation 6 dendrimer required an additional mobility mode to account for its nonterminal behavior. Since the required ultralow relaxation mode lasts longer than the longest molecular relaxation time

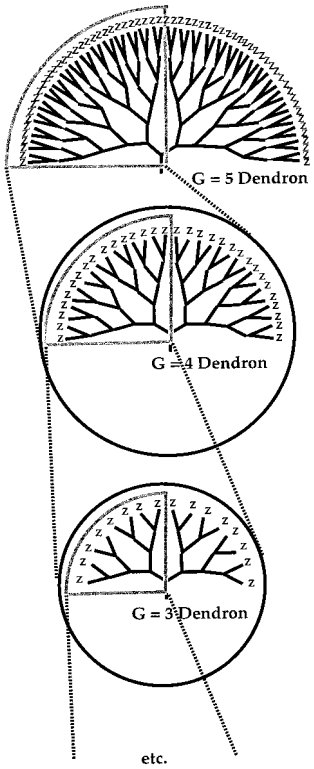

Figure 14. Schematic representation of a possible hierarchical order of potential rheological kinetic units in bulk flow of higher generation EDA−core PAMAM dendrimers.

(as identified approximately from the crossover of G' and G''), this indicates the existence of a structure that is larger than an individual dendrimer molecule. The nature of this structure, however, cannot be identified on the basis of these data alone.

Following the rationale of the Rouse model, the behavior of higher-generation dendrimers suggests the existence of more than one submolecular mode of stress relaxation (specifically 2, 9, and 15 for generations 4, 5, and 6, respectively). This seems to indicate that at generation 4 the dendrimer molecule may become too large to move coherently through the bulk as a single kinetic unit. Instead, two relaxation times exhibited by this dendrimer could correspond to elastic deformation of its individual dendrons and to the motions of their halves, which in turn are equivalent to generation-3 dendrons. Similarly, nine Rouse relaxation modes of generation-5 dendrimer (see Figure 14) may be associated with the motions of its whole dendrons and eight different subdendrons, the sizes of which are equivalent to the whole dendrons of generations 4, 3, and so on. Notably, this is in clear contrast to the behavior of these same PAMAM dendrimers in medium and concentrated solutions, where only the whole molecules were the kinetic flow units.[1] This difference is probably due to expanded conformation(s) that solvated dendrimers assume and/or a certain degree of solvent-induced shielding of *inter*dendrimer interactions.

An analysis of free volume of PAMAM dendrimers in the bulk revealed a generational dependence that is consistent with the previously observed change of their glass temperatures.[4,16−18] In addition, this change is also consistent with the qualitative conformational change of PAMAM dendrimer molecules at about generation 4 and with the soft interior−hard shell model of the dendrimer *intra*molecular morphology.[6]

Acknowledgment. This work was supported in part by Dendritech, Inc., Midland, MI, and the U.S. Army Research Laboratory Collaborative Research Program on Dendritic Polymers. Very helpful discussions with and suggestions by Professors Hans-Georg Elias of Michigan Molecular Institute are gratefully acknowledged. F.A.M also acknowledges the 3M Company for support during her sabbatical leave when some of this work was performed.

References and Notes

(1) Uppuluri, S.; Keinath, S. E.; Tomalia, D. A.; Dvornic, P. R. *Macromolecules* **1998**, *31*, 4498.
(2) Hawker, C. J.; Farrington, P. J.; Mackay, M. E.; Wooley, K. L.; Frechet, J. M. J. *J. Am. Chem. Soc.* **1995**, *117*, 4409.
(3) Dvornic, P. R.; Tomalia, D. A. *Sci. Spectra* **1996** (5), 36.
(4) Uppuluri, S. Ph.D. Thesis, Michigan Technological University, Houghton, MI, 1997.
(5) Prosa, T. K.; Bauer, B. J.; Amis, E. J.; Tomalia, D. A.; Scherrenberg, R. *J. Polym. Sci., Part B: Polym. Phys.* **1997**, *35*, 2913.
(6) Uppuluri, S.; Tomalia, D. A.; Dvornic, P. R. *Polym. Mater. Sci. Eng.* **1997**, *77*, 116.
(7) Dvornic, P. R.; Uppuluri, S.; Tomalia, D. A. *Polym. Mater. Sci. Eng.* **1995**, *73*, 131.
(8) Farrington, P. J.; Hawker, C. J.; Frechet, J. M. J.; Mackay, M. E. *Macromolecules* **1998**, *31*, 5043.
(9) Naylor, A. M.; Goddard, W. A., III.; Kiefer, G. E.; Tomalia, D. A. *J. Am. Chem. Soc.* **1989**, *111*, 2339.
(10) Mansfield, M. L.; Klushin, L. I. *J. Phys. Chem.* **1992**, *96*, 3994.
(11) Dvornic, P. R.; Tomalia, D. A. Dendritic Polymers. Divergent Synthesis, Starburst Poly(amidoamine) Dendrimers In *Polymeric Materials Encyclopedia*; Salamone, J. C., Ed.; CRC Press: Boca Raton, FL, 1996; Vol. 3, pp 1814−1830.
(12) Mattice, W. L. Masses, Sizes and Shapes of Macromolecules from Multifunctional Monomers. In Newkome, G. R.; Moorefield, C. N.; Vogtle, F. *Dendritic Molecules. Concepts, Synthesis, Perspectives*; VCH Verlag: Weinheim, Germany, 1996; Chapter I.
(13) Wege, V. U.; Grubbs, R. H. *Polym. Prepr.* **1995**, *36* (*2*), 239.
(14) Valachovic, D. E.; Bauer, B. J.; Amis, E. J.; Tomalia, D. A. *Polym. Mater. Sci. Eng.* **1997**, *77*, 230.
(15) Prosa, T. J.; Bauer, B. J.; Topp, A.; Amis, E. J.; Scherrenberg, R. *Polym. Mater. Sci. Eng.* **1998**, *79*, 307.
(16) Stutz, H. *J. Polym. Sci., Part B: Polym. Phys.* **1995**, *33*, 333.
(17) Wooley, K. L.; Hawker, C. J.; Pochan, J. M.; Frechet, J. M. J. *Macromolecules* **1993**, *26*, 1514.
(18) de Brabander-van der Berg, E. M. M.; Nijenhuis, A.; Mure, M.; Keulen, J.; Reintjens, R.; Vandenbooren, F.; Bosman, B.; de Raat, R.; Frijns, T.; Wal, S. V. D.; Castelijns, M.; Put, J.; Meijer, E. W. *Macromol. Symp.* **1994**, *77*, 51.
(19) Dvornic, P. R.; de Leuze-Jallouli, A. M.; Owen, M. J.; Perz, S. V. *Polym. Prepr.* **1998**, *39* (*1*), 473.
(20) Dvornic, P. R.; de Leuze-Jallouli, A. M.; Owen, M. J.; Perz, S. V. *Silicones in Coatings II*; Paint Research Association: London, UK, 1988.
(21) Dvornic, P. R.; de Leuze-Jallouli, A. M.; Owen, M. J.; Perz, S. V. Radially Layered Poly(amidoamine-organosilicon) (PAMAMOS) Copolymeric Dendrimers In *Silicones and Silicone-Modified Materials*, Clarson, S. J., Owen, M. J., Fitzgerald, J. J., Smith, S. D., Eds.; ACS Symposium Series Vol. 729; American Chemical Society: Washington, DC, 2000; Chapter 16, pp 241−269.
(22) Dvornic, P. R.; de Leuze-Jallouli, A. M.; Owen, M. J.; Perz, S. V. *Polym. Prepr.* **1999**, *40* (1), 408.
(23) Uppuluri, S.; Morrison, F. A.; Dvornic, P. R. 70th Annual Meeting of the Society of Rheology, Monterey, CA, Oct 4−8, 1998; Book of Abstracts, p 11.
(24) Tomalia, D. A.; Baker, H.; Dewald, J. R.; Hall, M. J.; Kallos, G.; Martin, S. J.; Roeck, J.; Ryder, J.; Smith, P. B. *Polym. J.* (*Tokyo*) **1985**, *17*, 117.
(25) (a) Berry, G. C.; Fox, T. G. *Adv. Polym. Sci.* **1968**, *5*, 261. (b) Kumar, N. G. *J. Polym. Sci., Macromol. Rev.* **1980**, *15*, 255. (c) Aharoni, S. M. *J. Appl. Polym. Sci.* **1977**, *21*, 1323. (d) Graessley, W. W. *J. Chem. Phys.* **1967**, *47*, 1942.
(26) Ferry, J. D. *Viscoelastic Properties of Polymers*, 3rd ed.; Wiley: New York, 1980.
(27) Cox, W. P.; Merz, E. H. *J. Polym. Sci.* **1958**, *28*, 619.
(28) Larson, R. G. *Constitutive Equations for Polymer Melts*; Butherworth: Stoneham, MA, 1988; pp 46−53.
(29) Pearson, D. S.; Helfand, E. *Macromolecules* **1984**, *17*, 888.
(30) Williams, M. L.; Landel, R. F.; Ferry, J. D. *J. Am. Chem. Soc.* **1955**, *77*, 3701.
(31) Vinogradov, G. V.; Malkin, A. Ya. *Rheology of Polymers*; Mir Publishers: Moscow, USSR, 1980.
(32) Aklonis, J. J.; MacKnight, W. J.; Shen, M. *Introduction to Polymer Viscoelasticity*; Wiley-Interscience: New York, 1972; p 67.
(33) Reference 26, p 288.
(34) Reference 26, Table 11-II, p 277.
(35) Mewis, J.; Macosco, C. W. Suspension Rheology. In *Rheology. Principles. Measurements and Applications*; Macosco, C. W., Ed.; VCH Publishers: New York, 1994; Chapter 10, pp 425−474.
(36) Lescanec, R. L.; Muthukumar, M. *Macromolecules* **1990**, *23*, 2280.
(37) Reference 28, pp 40−45.
(38) Ongi, S.; Jujji, T.; Kato, H.; Ogihara, S. *J. Phys. Chem.* **1964**, *68*, 1598.

MA990634U